Received: 4 November 2020 | Revised: 11 January 2021 | Accepted: 14 January 2021

DOI: 10.1002/bmc.5075

RESEARCH ARTICLE

Biomedical Chromatography WILEY

Comprehensive insights into the formation of metabolites of the ghrelin mimetics capromorelin, macimorelin and tabimorelin as potential markers for doping control purposes

Tobias Lange[1] | Andreas Thomas[1] | Christian Görgens[1] | Martin Bidlingmaier[2] | Katharina Schilbach[2] | Eric Fichant[3] | Philippe Delahaut[3] | Mario Thevis[1,4]

[1]Center for Preventive Doping Research/ Institute of Biochemistry, German Sport University Cologne, Am Sportpark Müngersdorf 6, Cologne, 50933, Germany

[2]Endocrine Laboratory, Medizinische Klinik und Poliklinik IV, Klinikum der Universität München, Ziemssenstraße 1, Munich, 80336, Germany

[3]Département Santé, CER Groupe, Rue du Point du Jour 8, Marloie, 6900, Belgium

[4]European Monitoring Center for Emerging Doping Agents, Am Sportpark Müngersdorf 6, Cologne, 50933, Germany

Correspondence
Mario Thevis, Center for Preventive Doping Research/Institute of Biochemistry, German Sport University Cologne, Am Sportpark Müngersdorf 6, Cologne, 50933, Germany.
Email: m.thevis@biochem.dshs-koeln.de

Funding information
Federal Ministry of the Interior, Building and Community (Berlin, Germany); Manfred-Donike-Institute for Doping Analysis (Cologne, Germany); World Anti-Doping Agency (Montreal, Canada), Grant/Award Number: #18A03MT

Abstract

Analytical methods to determine the potential misuse of the ghrelin mimetics capromorelin (CP-424,391), macimorelin (macrilen, EP-01572) and tabimorelin (NN703) in sports were developed. Therefore, different extraction strategies, i.e. solid-phase extraction, protein precipitation, as well as a "dilute-and-inject" approach, from urine and EDTA–plasma were assessed and comprehensive *in vitro*/*in vivo* experiments were conducted, enabling the identification of reliable target analytes by means of high resolution mass spectrometry. The drugs' biotransformation led to the preliminary identification of 51 metabolites of capromorelin, 12 metabolites of macimorelin and 13 metabolites of tabimorelin. Seven major metabolites detected in rat urine samples collected post-administration of 0.5–1.0 mg of a single oral dose underwent in-depth characterization, facilitating their implementation into future confirmatory test methods. In particular, two macimorelin metabolites exhibiting considerable abundances in post-administration rat urine samples were detected, which might contribute to an improved sensitivity, specificity, and detection window in case of human sports drug testing programs. Further, the intact drugs were implemented into World Anti-Doping Agency-compliant initial testing (limits of detection 0.02–0.60 ng/ml) and confirmation procedures (limits of identification 0.18–0.89 ng/ml) for human urine and blood matrices. The obtained results allow extension of the test spectrum of doping agents in multitarget screening assays for growth hormone-releasing factors from human urine.

KEYWORDS
anti-doping, ghrelin mimetics, *in vitro*/*in vivo* metabolism, LC–HRMS/MS

1 | INTRODUCTION

The ghrelin receptor agonists or ghrelin mimetics capromorelin (CP-424,391), macimorelin (macrilen, EP-01572) and tabimorelin (NN703) are included in the Prohibited List of the World Anti-Doping Agency (WADA, 2020), categorized as growth hormone secretagogues (GHS). Like the growth hormone releasing peptides (GHRPs), which also act as agonists of the ghrelin receptor, the GHS are classified as nonthreshold substances under section S2 "peptide hormones, growth factors, related substances, and mimetics" and prohibited at

all times, i.e. in and out of competition. These synthetic selective ligands of the ghrelin receptor, which is located in the hypothalamus and commonly referred to as the GHS receptor, were originally developed for the treatment of growth hormone (GH) deficiency (Cordido, Isidro, Nemina, & Sangiao-Alvarellos, 2009; Moulin, Ryan, Martinez, & Fehrentz, 2007). Owing to the stimulation of GH and insulin-like growth factor I (IGF-I), these peptidomimetic drugs possess considerable potential for misuse in sports, as supported by 26 adverse analytical findings reported in 2019 for GHRPs and GHS (WADA, 2019a) and, consequently, it is critical to continuously update and improve detection methods for these substances.

All three compounds considered in this study are orally active GHS receptor agonists. Since the tripeptidyl derivative tabimorelin was found to have only modest clinical effects in adults with GH deficiency (Svensson et al., 2003) and functioned as an inhibitor of CYP3A4 with associated undesirable interactions (Zdravkovic et al., 2003), US Food and Drug Administration (FDA) approval was not achieved. The modified dipeptide capromorelin slightly increased total lean body mass and physical performance in elderly men (White et al., 2009), but the effects were not considered sufficient to conduct follow-up studies. Instead, the drug was approved by the FDA for appetite stimulation in dogs (Rhodes, Zollers, Wofford, & Heinen, 2018). In 2017, tripeptidyl derivative macimorelin received FDA approval for the purpose of GH deficiency diagnosis (stimulation test).

The therapeutic dosing combined with short half-lives for tabimorelin (4.1 ± 0.4 h in swine) (Hansen et al., 1999), capromorelin (2.5 ± 0.4 h at 50 mg dosage; Ellis et al., 2015) and macimorelin (1.9 ± 0.3 h at 0.25 mg/kg dosage; Piccoli et al., 2007) might pose a challenge for the sensitive detection of illicit applications. Today, antidoping laboratories apply different sample preparation methods to target GHRPs/GHS in routine doping control samples, i.e. urine, plasma/serum and dried blood spots, for initial testing procedures (ITP). In most cases, the "dilute-and-inject" (D&I) approach (Goergens, Guddat, Thomas, & Thevis, 2018; Judak, Grainger, Goebel, Van Eenoo, & Deventer, 2017; Kwok et al., 2020; Thomas et al., 2016) or purification and concentration using solid-phase extraction (Guan, You, Li, & Robinson, 2019; Kim et al., 2018; Lange, Thomas, Walpurgis, & Thevis, 2020; Pugliese, Boyce, Lawler, Coumbaros, & Le, 2019) were preferred for LC–MS/MS-based analytical approaches.

In the past, *in vitro* experiments using serum/plasma, human liver microsomes, S9 fractions and *in vivo* experiments with human and rat model were successfully applied to identify various biotransformation products of administered (pseudo)peptides as demonstrated for GHRPs (Esposito, Deventer, Geldof, & Van Eenoo, 2015; Okano, Sato, Ikekita, & Kageyama, 2010; Thomas, Delahaut, Krug, Schänzer, & Thevis, 2012; Thomas, Knoop, Schanzer, & Thevis, 2017). In order to optimize detection assays with regards to specificity, sensitivity and retrospectivity, such metabolites are commonly included into the list of target analytes. For instance, the metabolites of GHRP-1, GHRP-2, alexamorelin, hexarelin and ipamorelin offered superior detection windows compared with the intact drugs/drug candidates (Okano, Sato, Ikekita, & Kageyama, 2010; Semenistaya et al., 2015; Thomas et al., 2011; Thomas, Delahaut, Krug, Schaenzer, & Thevis, 2012; Timms, Hall, Levina, Vine, & Steel, 2014; Zvereva, Semenistaya, Krotov, & Rodchenkov, 2016). In contrast to the GHRPs and their metabolites, tabimorelin, capromorelin and macimorelin are compounds of lower molecular mass (<600 Da) and feature rather nonpeptidic characteristics. Therefore, the main metabolic transformation reactions are expected to occur in liver and kidney tissues, catalyzed by enzymes with relatively low substrate specificity such as cytochromes P450 (CYPs).

Recently, Sobolevsky et al. reported a multiclass ITP including the detection of capromorelin, macimorelin and tabimorelin in human urine (Sobolevsky & Ahrens, 2020). However, detection methods from both matrices, i.e. blood plasma and urine, as well as confirmation procedures (CP) and information about the formed metabolites of these drugs are still missing. Therefore, the focus of this work was the identification of metabolites using different *in vitro*/*in vivo*/*in silico* approaches. In addition, using efficient extraction procedures for both matrices, adequate analytical detection methods for the analysis of the intact drugs by LC–HRMS/MS should be established. Samples and data on the compounds' metabolism were obtained by *in vivo* (rat) and *in vitro* (human liver microsomes and human serum incubation) experiments. The identification of metabolites was assisted by software prediction and *in silico*-generated data (Djoumbou-Feunang et al., 2019a; Zaretzki, Matlock, & Swamidass, 2013), and MS/MS-based metabolite structural elucidations were supported by utilizing competitive fragmentation modeling ("CFM-ID 3.0") via a freely available web server (Djoumbou-Feunang et al., 2019b).

2 | MATERIALS AND METHODS

2.1 | Chemicals and materials

The analytes of this study, capromorelin (L)-tartrate {2-amino-*N*-[(1*R*)-2-[(3a*R*)-2,3,3a,4,6,7-hexahydro-2-methyl-3-oxo-3a-(phenylmethyl)-5H-pyrazolo[4,3-c]pyridin-5-yl]-2-oxo-1-propanamide (2*R*,3*R*)-2,3-dihydroxybutanedioate} with a specified purity of 98.0% and tabimorelin {*N*-[(2*E*)-5-Amino-5-methyl-1-oxo-2-hexenyl]-*N*-methyl-3-(2-naphthalenyl)-D-alanyl-*N*,*Nα*-dimethyl-D-phenylalaninamide} with a specified purity of 98.7%, were purchased from Toronto Research Chemicals (North York, Ontario, Canada). Macimorelin acetate {2-amino-*N*-[(*R*)-1-{[(*R*)-1-formamido-2-(1H-indol-3-yl)ethyl]amino}-3-(1H-indol-3-yl)-1-oxopropan-2-yl]-2-methylpropanamide acetate} with a specified purity of 99.9% was obtained from NucleoSyn (Olivet, France). The internal standard (ISTD) (d_3)-GHRP-2 (1–3) metabolite (purity 72%) was synthesized in-house (Thomas et al., 2011) and (d_4)-GHRP-4 (purity >90%) was obtained from BMFZ (Düsseldorf, Germany). Chemicals for *in vitro* studies were pooled human liver microsomes from Sekisui XenoTech (Kansas City, KS, USA), β-nicotinamide adenine dinucleotide 2′-phosphate (NADPH) from Roche (Basel, Switzerland) and Na_2HPO_4 and NaH_2PO_4 from Merck (Darmstadt, Germany). Other chemicals that were used for sample preparation or as LC solvents were acetonitrile, methanol,

acetic acid and 25% (v/v) ammonia solution bought from Merck, formic acid obtained from Thermo Fisher Scientific (Waltham, MA, USA) and dimethyl sulfoxide (DMSO) supplied from Alfa Aesar (Haverhill, MA, USA). The Oasis mixed-mode cation exchange 1 cm^3 cartridges with 10 mg sorbent per unit were received from Waters (Milford, MA, USA).

2.2 | Standard solutions

The 1 mg/ml stock solutions of capromorelin, macimorelin, tabimorelin, (d_3)-GHRP-2 (1–3) metabolite and (d_4)-GHRP-4 were prepared with Milli-Q® water in LoBind tubes (Eppendorf, Hamburg, Germany) and stored at −20°C. Tabimorelin required an additional 20% of DMSO and 2% of acetic acid for complete solubilization. Immediately before each experiment, stock solutions were diluted with Milli-Q® water to obtain working solutions of the desired concentrations. Urine and plasma samples were fortified to the desired analyte concentration with 5% (v/v) of the working solution.

2.3 | *In vivo*, *in vitro* and *in silico* experiments

In order to study the metabolic profile of the drugs, different strategies were employed. *In vitro* incubation experiments with human serum or human liver microsomes and *in silico* predictions should confirm and complement the findings of the rat experiments as well as accelerate and facilitate the data analysis.

2.4 | *In vivo* experiments

Animal studies were conducted with approval of the local ethical committee and following the directive 2010/63/EU of the European Parliament and the Council of 22 September 2010 on the protection of animals used for scientific purposes. Six female brown rats (*Rattus norvegicus*, Wistar) with 200–300 g body weight received a single oral dose of 0.5 mg of capromorelin or tabimorelin, or 1 mg of macimorelin (two rats per drug). In addition, one rat not receiving any medication provided negative control test samples. The animals had free access to food and water. Urine samples of 1–13 ml were collected by means of a metabolic cage after 0, 6, 12, 24 and 36 h. Sample collections of blood with a volume of 2 ml each were performed after 0, 3, 12 and 36 h, yielding EDTA–plasma for the intended studies.

For urine sample preparation, 1 ml of rat urine with 2 ng of the ISTD mix was subjected to a generic SPE method (mixed-mode cation exchange cartridge) following the manufacturer's instructions for mixed-mode sorbents. For plasma sample preparation, a previous protocol for serum samples was adapted (Thomas, Delahaut, Krug, Schaenzer, & Thevis, 2012) and 100 µl of rat EDTA–plasma with 2 ng of the ISTD mix was subjected to protein precipitation with acetonitrile. The details of both protocols can be obtained from the Supplementary Information.

2.5 | *In vitro* experiments

The *in vitro* metabolism of capromorelin, macimorelin and tabimorelin was studied by incubation of the substrates with human serum and human liver microsomal preparations. As described in a previous study (Thomas, Knoop, Schanzer, & Thevis, 2017), 100 µl of human serum was fortified with 1 µg of each compound. For the production and identification of phase I metabolites using liver microsomes, a protocol from Knights, Stresser, Miners, & Crespi (2016) was adapted. A substrate blank (control) sample and an enzyme blank (control) sample were additionally prepared for both experiments. The details for the protocols can be found in the Supplementary Information.

2.6 | *In silico* experiments

The generation of various possible metabolites by software prediction provided a general insight into possible metabolic products of the drugs. The open-access software tool BioTransformer (Djoumbou-Feunang et al., 2019a) was operated with the task "metabolism prediction" and "human [tissues] and human gut microbial transformation". Three consecutive reaction steps were conducted. As input type a SMILES string was included. In addition, a similar approach was followed by the XenoSite web predictor tool (Zaretzki, Matlock, & Swamidass, 2013). A total of six different prediction systems (P450 metabolism, epoxidation, quinone formation, reactivity and UDP–glucuronosyltransferase metabolism) were chosen, and molecules were uploaded as MDL-molfiles. In contrast to BioTransformer, which provided proposed structures of the metabolites, this freely available tool predicted the atomic sites that could undergo metabolic modification. After applying both approaches, the putative metabolites generated were added to a target list (not shown) for further studies by LC–HRMS/MS of the *in vivo*/*in vitro* prepared samples.

2.7 | LC–HRMS/MS

The metabolites generated from *in vivo*/*in vitro* experiments were separated on a Vanquish UHPLC system (Thermo Fisher Scientific, Bremen, Germany) equipped with a Poroshell 120 EC-C_{18} analytical column, 3.0 × 50 mm, 2.7 µm particle size (Agilent Technologies, Santa Clara, CA, USA) and analyzed on an Orbitrap Exploris 480 MS (Thermo Fisher Scientific, Bremen, Germany). The supply of nitrogen (source and collision gas) was ensured by a nitrogen membrane generator (cmc Instruments, Eschborn, Germany). The 15 min LC run with flow rate of 350 µl/min and linear gradients was carried out with solvent A (ddH_2O and 0.1% formic acid) and solvent B (acetonitrile and 0.1% formic acid). In order to achieve ultimate sensitivities with regards to the limit of identification (LOI) and limit of detection (LOD) within the method validation, 1% DMSO was added to solvent B. The chromatographic gradient of the method started at 1% B and reached 40% B after 10 min. Subsequently, the organic phase (B) was increased to 90% in 0.5 min and held for 1.5 min before the analytical

column was re-equilibrated at 1% B for 3 min. The samples in the autosampler were kept at 10°C, while the analytical column was tempered to 30°C. The global MS settings using a heated electrospray ion (HESI) source were as follows: spray voltage (positive ion) at 3 kV, ion transfer tube temperature at 320°C, sheath gas at 30 arbitrary units, auxiliary gas at 10 arbitrary units, maximum spray current at 10 μA and vaporizer temperature at 300°C. For an in-depth characterization of the anticipated *N*-hydroxylation of a capromorelin metabolite, an atmospheric pressure chemical ionization (APCI) source was installed with the following experimental setup: spray voltage at 3 kV, ion transfer tube temperature at 275°C, sheath gas at 35 arbitrary units, auxiliary gas at 5 arbitrary units, maximum spray current at 4 μA and vaporizer temperature at 350°C. Full-scan HRMS experiments were acquired at an Orbitrap resolution (*r*) of 120,000 (FWHM at m/z = 200) with a scan range (m/z) from 120 to 1,200, a maximum injection time of 100 ms and an AGC target of 1×10^6. For structural elucidation and confirmation purposes, targeted MS^2 (tMS^2) experiments with an inclusion list of 1–4 entries and a quadrupole isolation window (m/z) of 1, and a retention time window of 1 min were applied. The MS^2 scans were acquired with r = 60,000, maximum injection time 100 ms, AGC target of 1×10^5 and stepped HCD collision with normalized collision energies (NCE) at 10, 20, and 40%. Optional pseudo MS^3 (pMS^3) experiments were conducted using the same settings but with an activated source-induced fragmentation voltage of 35 V and an inclusion list adapted accordingly. For initial testing purposes, a targeted SIM (tSIM) scan with inclusion list was performed at r = 60,000, a quadrupole isolation window (m/z) of 4, maximum injection time of 100 ms and AGC target of 1×10^5. The small number of analytes allowed alternating experiments of full HRMS, tMS^2 and tSIM scans between 7 and 12 min within the same method, controlled by Xcalibur version 4.3.

For the implementation of the three new compounds into the multitarget screening assay for GH-releasing factors from urine, the routinely applied LC–HRMS/MS-based testing procedure (Goergens, Guddat, Thomas, & Thevis, 2018) employing a Q Exactive™ Plus Hybrid Quadrupol–Orbitrap™ MS (Thermo Fisher Scientific, Bremen, Germany) was re-validated. Further, a Xevo TQ-XS mass spectrometer from Waters (Melford, MA, USA) was used for in-depth characterization of a metabolite of capromorelin. Details about the LC–TQMS/MS method can be found in the Supplementary Information in "Supplementary material and methods".

2.8 | Method validation

2.8.1 | Sample preparation

LC–HRMS/MS detection methods for the intact compounds were established and validated. Here, different method validation protocols were chosen, depending on whether urine or EDTA–plasma was used as test matrix. For urine, a D&I approach (Goergens, Guddat, Thomas, & Thevis, 2018) was used for the ITP and CP. Therefore, 90 μl of native urine was fortified with 10 μl of a 20 ng/ml ISTD working solution, mixed thoroughly and 40 μl was injected into LC–HRMS. In addition, a second CP approach by solid-phase extraction allowing utmost sensitivity and selectivity was adopted from the *in vivo* experiments as described above. The sample preparation for ITP and CP of plasma samples by protein precipitation with acetonitrile was conducted likewise as described previously in the protocol of the *in vivo* experiments.

2.8.2 | Validation for nonthreshold substances

The minimum required performance level (MRPL) for capromorelin, macimorelin and tabimorelin in urine is 2 ng/ml as specified by WADA. Although no regulatory specifications exist, the same MRPL was assumed for plasma samples. A total of five LC–HRMS/MS detection methods, i.e. an ITP and a CP for each matrix, plus an additional CP using SPE for urine, were validated according to WADA's International Standard for Laboratories 10.0 (WADA, 2019b). For fast and reliable initial testing purposes, tSIM experiments scanned for two diagnostic precursor ions originating from the intact compounds' protonated molecules' isotopes at the respective retention times. A presumptive adverse analytical finding triggers the CP. For confirmation purposes, three diagnostic precursor–product ion transitions were monitored by means of tMS^2 scans, all of which need to fulfill the criteria of signal-to-noise ratio >3 and relative retention time (rt_R) < 1% (to the ISTD signal). The precursor ion of each compound was identical to the tSIM ion 1 (see Table 2). For MS^2 identification, the transitions were additionally subjected to a maximum tolerance window for the relative abundance in a sample, relative to the base peak in a reference spectrum as specified in TD2015IDCR (WADA, 2015).

According to these criteria and following WADA guidelines, the validation of the qualitative ITPs and CPs were carried out for the parameters selectivity, repeatability, robustness, carryover, LOD and LOI.

2.8.3 | Validation parameters

For the assessment of selectivity of the ITP, 10 different urine blank and EDTA–plasma blank samples (female n = 5 and male n = 5) were analyzed with the particular MS method. Repeatability of detection at MRPL (ITP) was evaluated by analyzing the same set of samples, fortified with an analyte concentration of 2 ng/ml. For the estimation of the LOD (ITP), six different urine and plasma samples were fortified at 1% MRPL (0.02 ng/ml), 10% MRPL (0.2 ng/ml), 25% MRPL (0.5 ng/ml), 50% MRPL (1 ng/ml) and 100% MRPL (2 ng/ml). The LOD was defined as the lowest concentration of a compound with a 95% detection rate, calculated using a detection response curve according to the WADA's International Standard for Laboratories 10.0. (WADA, 2019b). The carryover of the ITP was evaluated by analyzing a blank sample directly after a sample containing a high concentration of 400% MRPL (8 ng/ml). A re-analysis of the "repeatability samples" at the MRPL was used to test whether the sample extracts were

stable in the autosampler over a longer period of time (24 h). With regard to the diagnostic ion transitions, similar validation parameters were predetermined for the CPs. Selectivity and carryover were subjected to the same requirements as for the ITP. The LOI, again at 95% identification rate, was calculated with the same series of the MRPL levels as for the LOD estimation before, yet must meet the identification criteria of a CP. LC–HRMS method robustness was verified during the series of measurements for LOI estimation and a batch of six samples of 100% MRPL ("D&I" from urine and "PP" from plasma) and 50% MRPL ("SPE" from urine) were prepared and analyzed again on a different day.

3 | RESULTS AND DISCUSSION

3.1 | *In vivo*, *in vitro*, and in silico experiments

Prior to the metabolite screening, the intact, unmodified compounds were monitored, identified and characterized by LC–HRMS/MS. In the upper panel of Figure 1a–c, the extracted ion chromatograms of a rat urine sample at 0 and 6 h post-administration of the respective drug—capromorelin (a), macimorelin (b) and tabimorelin (c)—are shown with the obtained isotopic patterns of the detected protonated molecules. A corresponding MS^2 spectrum of the $[M + H]^+$ ion at NCE of 20% is provided in the middle panel. As indicated, several fragments and neutral losses were tentatively assigned by fragmentation modeling via CFM-ID 3.0 taking a set of three input MS^2 spectra at NCE of 10, 20 and 40%. As demonstrated in the lower panel, all substances reached their maximum concentration 6 or 3 h post-administration in urine or EDTA–plasma (data not shown), respectively. In rat urine, the drugs were still detected at the end of sample collection at 36 h. Although of considerably lower concentration in EDTA–plasma samples, capromorelin and tabimorelin were also still detectable at the end of the sample collection period. In contrast, signals corresponding to macimorelin were only detectable in plasma samples collected 3 h post-administration. The excretion half-lives for the tested drugs in rats as estimated from the available urine samples were ~7.5 h for capromorelin, ~3 h for macimorelin and ~5 h for

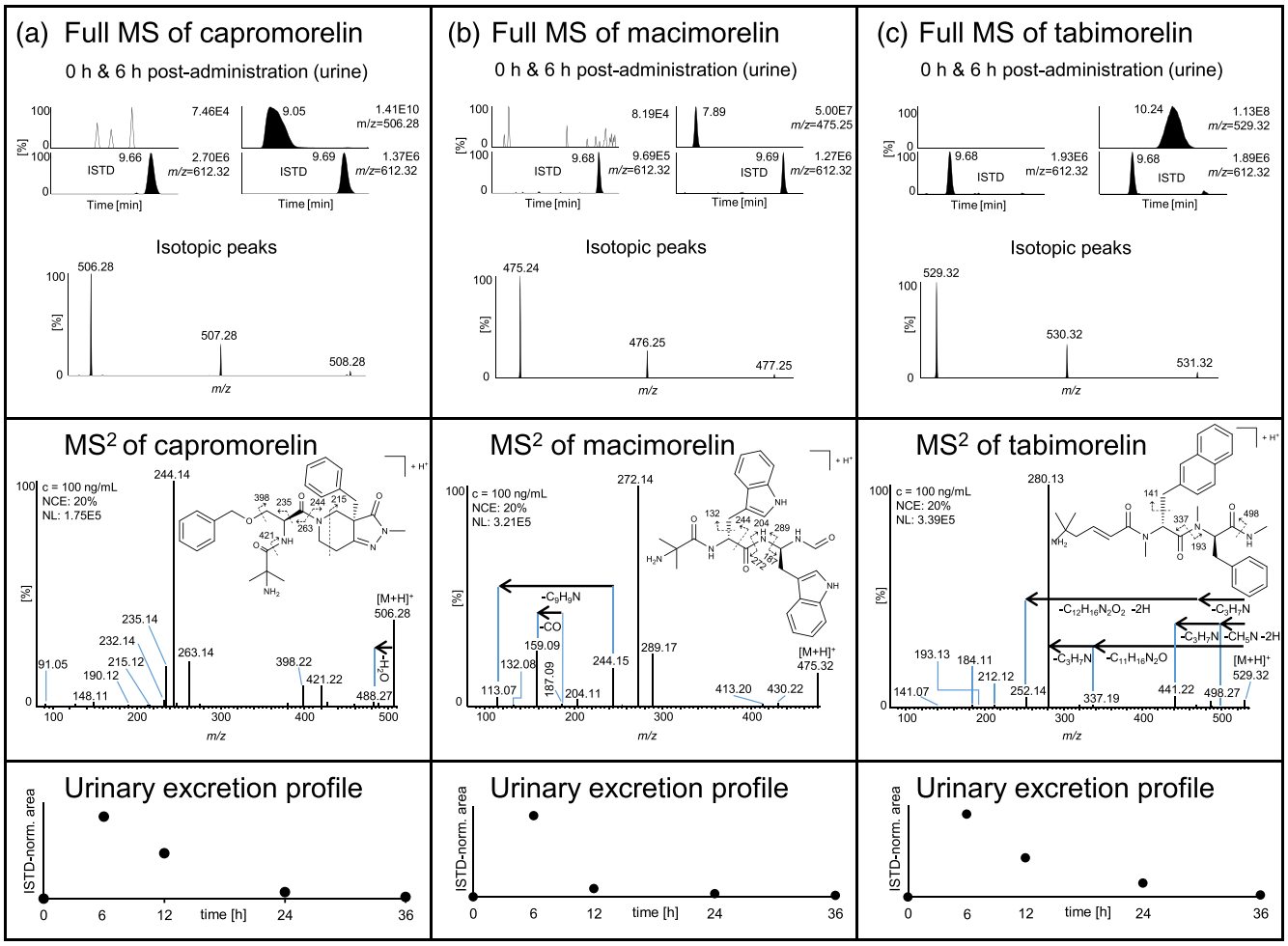

FIGURE 1 In the upper panel, the extracted ion chromatogram (mass tolerance ±5 ppm) of a full HRMS experiment of capromorelin (a), macimorelin (b) and tabimorelin (c) at 0 and 6 h post-administration is shown. The corresponding isotope signals are shown in the mass spectrum below. The middle panel contains a MS^2 spectrum of the reference compound (c = 100 ng/ml). The lower panel shows the drug's urinary excretion profile in rat

tabimorelin. The estimated plasma half-lives, albeit only based on four data points, were 3.5 h for capromorelin and 5.5 h for tabimorelin and are in agreement with other studies in human or swine as mentioned above (Ellis et al., 2015; Hansen et al., 1999). Among these substances, the shortest (human) plasma half-life was reported for macimorelin ($t_{1/2}$ = 1.9 h; Piccoli et al., 2007), which may have also complicated the detection in rat EDTA–plasma in the present study. Whether certain metabolites of these drugs would eventually allow for a longer detection window compared was the intact compound and could increase the assay's sensitivity or specificity was subsequently investigated.

The strategy for identifying metabolites consisted of the targeted scanning for isotopic masses (5 ppm accuracy) in full HRMS scans. The list of putative metabolites was generated beforehand by a combination of different *in silico* experiments and metabolite predictions. The metabolic fate of the drugs resulted in a whole range of different phase I and phase II metabolites. Considering all *in vivo*/*in vitro* experiments, a total of 51 capromorelin metabolites, 12 macimorelin metabolites and 13 tabimorelin metabolites were detected. They were found predominantly in rat urine, rat EDTA–plasma, and human microsomal preparations, and partially also using human serum incubation experiments. A set diagram showing the number of metabolites of capromorelin (a), macimorelin (b), and tabimorelin (c), detected by full HRMS experiments, is depicted in Figure 2. The overlapping sets represent the shared metabolites from two or all four different matrices and/or *in vitro*/*in vivo* approaches. By far the most urinary phase I and phase II metabolites were found for capromorelin (45), followed by macimorelin (10) and tabimorelin (5). In rat EDTA–plasma, significantly fewer metabolites were observed for capromorelin (11) and none for macimorelin and tabimorelin. The *in vitro* (human microsomes) experiments revealed several phase I metabolites for capromorelin (19), macimorelin (7) and tabimorelin (10). Also the *in vitro* incubation with human serum yielded metabolic products for capromorelin (7), macimorelin (7) and tabimorelin (1). In accordance with the fact that mainly CYPs and UDP–glucuronosyltransferases are enriched in the liver microsomes, a high diversity and abundance of hydroxy metabolites was observed. Phase II conjugates were not identified in microsomal preparations because of the lack of an additional cofactor (UDP–glucuronic acid). Other metabolites, however, were less concentrated and diverse than in the *in vivo* studies (urine). Of note, the evaluation of the enzyme blank control samples of both *in vitro* assays demonstrated that 47% (liver microsomes) and 67% (human serum) of the obtained metabolites were also produced, albeit with partially reduced signal intensities, suggesting, e.g., spontaneous oxidations or environmental microbial transformation during sample preparation and/or incubation.

Within anti-doping research projects for GHRP metabolite identification, it has already been demonstrated that urinary metabolites detected for a rat model (Thomas, Delahaut, Krug, Schänzer, & Thevis, 2012) could also be determined in human urine after nasal administration (Semenistaya et al., 2015). Here, assuming a similar transferability from the animal model to humans, the main focus was on the rat *in vivo* experiments. An overview of the urinary metabolites observed in full HRMS data obtained from rat 6 h post-administration of capromorelin (a), macimorelin (b) and tabimorelin (c) is shown in Figure 3.

As demonstrated here, the metabolite profiles of the analytes were different in the number and abundance of metabolites and yet some similarities existed. At least for the rat urine collected 6 h post-administration, the metabolite concentrations were below those of their precursor compounds. Capromorelin, macimorelin and tabimorelin were all prone to CYP-mediated mono(/di)-hydroxylation/epoxidation and *N*-dealkylation, resulting in several phase I metabolites. Furthermore, phase II metabolites such as *O*/*N*-glucuronidated metabolites were detected for the three drugs.

The thorough characterization of the most abundant urinary metabolites was completed with subsequent complementary experiments by tMS^2, pMS^3, neutral loss scan, precursor ion scan or the temporary use of an APCI source instead of a HESI source. Finally, a list of the major metabolites of each compound was established with the prerequisite of reaching a relative (to the unmodified compound) abundance of at least >1% at any given sample collection time or matrix.

Table 1 contains the main analytical characteristics of each metabolite, e.g. molecular formula, t_R (min), predominant charge state and isotope signals (*m*/*z*). As the individual drugs showed unique

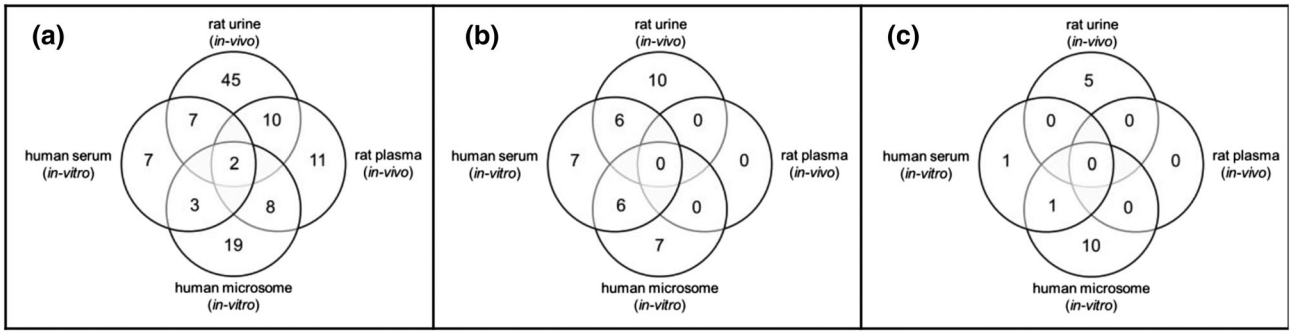

FIGURE 2 A set diagram showing the number of metabolites of capromorelin (a), macimorelin (b) and tabimorelin (c), detected by full HRMS experiments. The overlapping sets represent the shared metabolites from two or all four different matrices and/or different *in vitro*/*in vivo* approaches

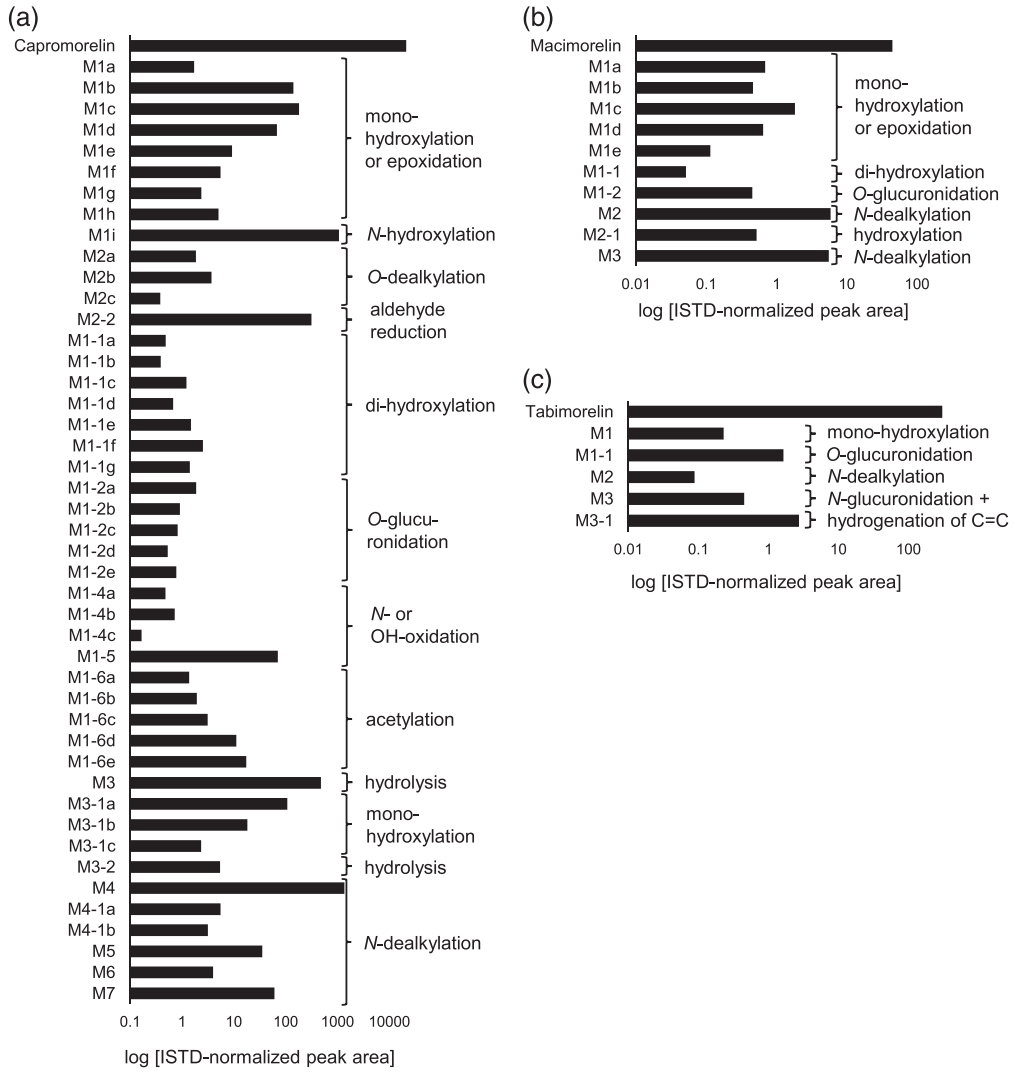

FIGURE 3 Overview of all metabolites (M) found in the drug-administered rat urine 6 h post-administration of (a) capromorelin, (b) macimorelin and (c) tabimorelin. The assumed chemical or enzymatic reactions that formed a metabolite are indicated on the right

metabolite profiles *in vivo*/*in vitro*, these were presented in separate sections. Here, the focus was on the major rat urinary metabolites; however, various minor metabolites were additionally characterized and described (see Supplementary Information, Figs S1 and S21 and Tables S1–S3).

3.2 | Capromorelin

The interpretation of the full HRMS scan revealed 45 metabolites detected in rat urine (Figure 2a), 11 metabolites detected in rat EDTA–plasma, 19 metabolites detected in microsome incubated drug samples and seven metabolites detected after human serum incubation. Subsequent MS characterization and monitoring of the urinary excretion profile were accomplished for the most abundant metabolites observed in rat urine. In comparison with the intact drug, the amount of traceable capromorelin metabolites was relatively low, independent of the *in vitro* or *in vivo* experiments conducted. The three most abundant metabolites (M) detected in rat urine and, therefore, the most interesting ones with regards to sports drug testing were the hydroxylamine M1i (Figure 4), the hydrolyzed M3 (Figure 5), and the *N*-dealkylated M4 (Figure S2).

In rat urine, between t_R 6.67 and 10.03 min, at least nine different metabolites (M1a–i), presumably originating from CYP-mediated mono-hydroxylation or epoxidation, were observed by full HRMS (Figure 4a, upper panel) and characterized by tMS^2 experiments. The majority of them, eluting between t_R 6.67 and 8.39 min, contain the introduced hydroxy group (or epoxide) within the left or right benzyl moiety, ascertained by respective diagnostic product ions (data not shown). The main hydroxylated metabolite, found in rat urine 6–36 h post-administration, in rat EDTA–plasma 3 h post-administration, and in human microsomal preparations (*in vitro*), was the putative hydroxylamine M1i, eluting at 10.03 min. In contrast to the most C-hydroxylated metabolites, the biotransformation from amines to

TABLE 1 Overview of the most abundant metabolites of capromorelin, macimorelin and tabimorelin detected after *in vivo* or *in vitro* experiments

Compound	Molecular formula	t_R (min)	Charge state	Isotope 1 Isotope 2 Isotope 3 (*m/z*)	Reaction type	Compound detected in: (1) rat EDTA–plasma (*in vivo*); (2) rat urine (*in vivo*); (3) human microsomes (*in vitro*); (4) human serum (*in vitro*)
Capromorelin	$C_{28}H_{35}N_5O_4$	9.05	1+	506.2762 507.2795 508.2829	—	(1) 3–36 h post-administration (2) 6–36 h post-administration (3) S, E + S (4) S, E + S
Capromorelin M1i	$C_{28}H_{35}N_5O_5$	10.03	1+	522.2711 523.2745 524.2778	*N*-Hydroxylation	(1) 3–12 post-administration (2) 6–36 h post-administration (3) E + S (4) No signal
Capromorelin M3	$C_{24}H_{29}N_4O_3$	8.77	1+	421.2234 422.2265 423.2293	Hydrolysis of amide	(1) 3–36 h post-administration (2) 6–36 h post-administration (3) S, E + S (4) S, E + S
Capromorelin M4	$C_{27}H_{33}N_5O_4$	8.37	1+	492.2605 493.2639 494.2672	*N*-Dealkylation	(1) 3–12 h post-administration (2) 6–36 h post-administration (3) S, E + S (4) S, E + S
Macimorelin	$C_{26}H_{30}N_6O_3$	7.89	1+	475.2452 476.2486 477.2519	—	(1) 3 h post-administration (weak signal) (2) 6–36 h post-administration (3) S, E + S (4) S, E + S
Macimorelin M1c	$C_{26}H_{30}N_6O_6$	6.83	1+	491.2401 492.2435 493.2468	Hydroxylation	(1) No signal (2) 6–12 h post-administration (3) S, E + S (4) S, E + S
Macimorelin M2	$C_{15}H_{20}N_4O_2$	4.62	1+	289.1659 290.1693 291.1726	*N*-Dealkylation	(1) No signal (2) 6–36 h post-administration (3) S, E + S (4) S, E + S
Macimorelin M3	$C_{11}H_{10}N_{2O}$	4.16	1+	187.0866 188.0899 189.0933	*N*-Dealkylation	(1) no signal (2) 6–36 h post-administration (3) E + S (weak signal) (4) No signal
Tabimorelin	$C_{32}H_{40}N_4O_3$	10.24	1+	529.3173 530.3207 531.3240	—	(1) 3–12 h post-administration (2) 6–36 h post-administration (3) S, E + S (4) S, E + S
Tabimorelin M3-1	$C_{38}H_{50}N_4O_9$	8.65	1+	707.3579 708.3612 709.3647	*N*-Glucuronidation, hydrogenation of C=C	(1) No signal (2) 6–24 h post-administration (3) E + S (weak signal) (4) No signal

t_R, Retention time; S, substrate incubated; E, enzyme incubated.

hydroxylamine or *N*-oxide metabolites frequently results in an increased retention time on reversed-phase LC under acidic conditions (Fitch, He, Tu, & Alexandrova, 2007; Miller, Doss, & Stearns, 2004; Qi, Wu, Cheng, & Qu, 2009). A number of further indications substantiated the proposed structure of this metabolite. First, as observed in the MS^2 spectrum of the $[M + H]^+$ ion at *m/z* = 522.2711, the additional accurate mass of an oxygen atom (15.9944 u) was neither located at the benzyl moieties nor at the hexahydropyrazolopyridine residue of the molecule (Figure 4b). Second, the abundance of the ion at *m/z* = 522.2711 was not affected by employing APCI instead of ESI, which would be expected in case of *N*-oxides owing to the reported thermal instability during APCI (Ramanathan et al., 2000). Third, the pMS^3 mass spectrum of *m/z* 522.2711 → 421.2233 (Figure S3), representing the precursor capromorelin minus the *N*-terminal α-methylalanine residue, confirmed the absence of a hydroxyl group in this structural part of the metabolite. Furthermore, *m/z* = 421.2233 also represents the hydrolyzed capromorelin M3, identified at t_R 8.77 min

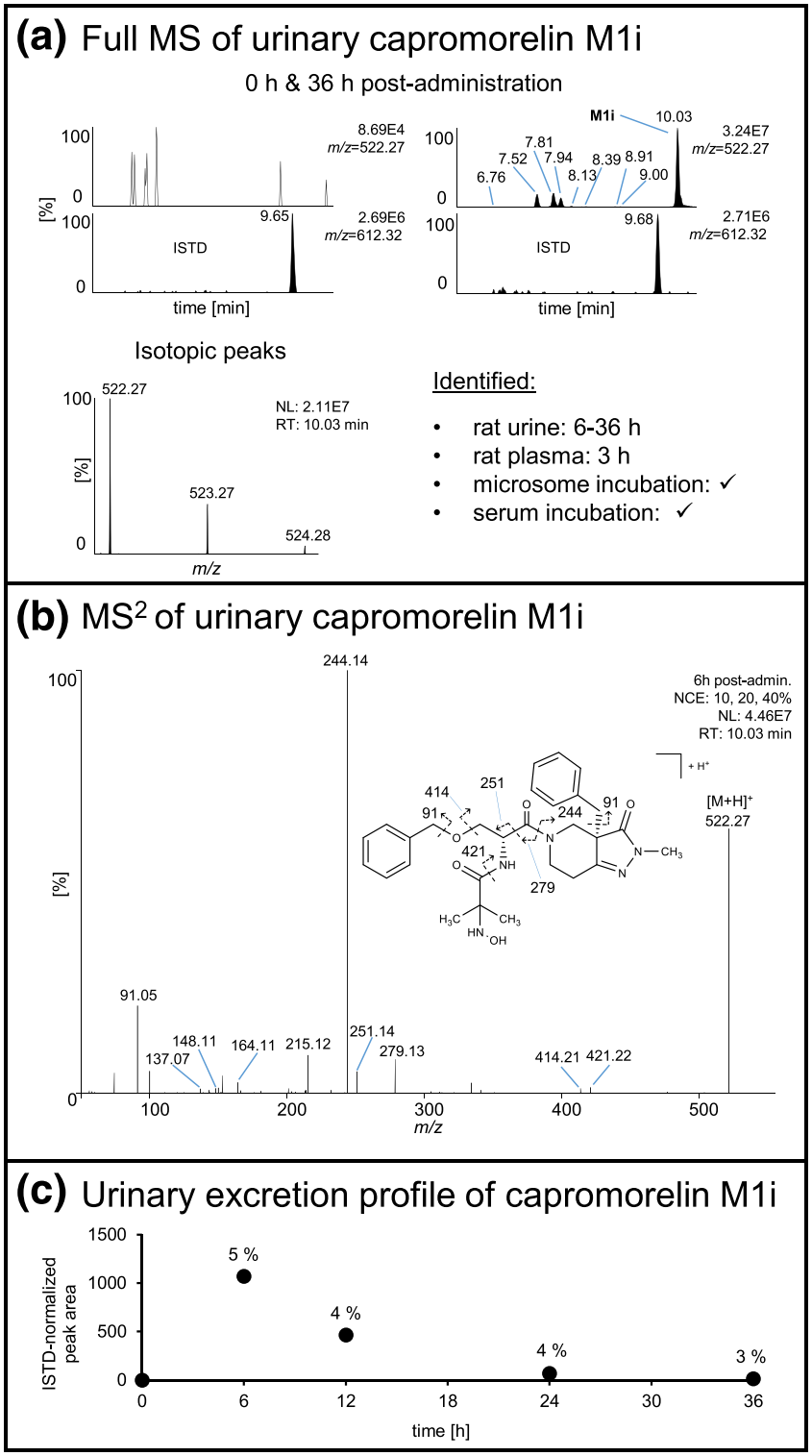

FIGURE 4 (a) The extracted ion chromatogram (mass tolerance ±5 ppm) of the full HRMS of the urinary capromorelin hydroxylamine M1i with the $[M + H]^+$ ion of m/z = 522.2711 at 0 and 36 h post-administration and, below, the isotope signals of the mass spectrum at retention time, t_R, 10.03 min (36 h post-administration). (b) The MS^2 spectrum of the $[M + H]^+$ ion of a sample collected 6 h post-administration. (c) The urinary excretion profile with the indicated percentages referring to the relative abundance of the ISTD-normalized peak area

(Figure S5a) and its MS^2 mass spectrum (Figure 5b) was in good agreement with the pMS^3 mass spectrum of m/z 522.2711 → 421.2233. In contrast, the pMS^3 mass spectrum of m/z 522.2711 → 279.1337, representing (*Z*)-2-amino-*N*-(1-[benzyloxy]-3-oxoprop-1-en-2-yl)-2-methylpropanamide (Figure S4), showed the neutral losses of CO (27.9949 u) and C_3H_7NO (73.0528 u), with the latter indicating *N*-(prop-1-en-2-yl)hydroxylamine or 2-aminoprop-2-en-1-ol. The product ion mass spectrum of an additional pMS^3 experiment at m/z 522.2711 → 251.1390, representing (*Z*)-2-amino-*N*-(2-[benzyloxy] vinyl)-2-methylpropanamide (Figure S5), was in good agreement with the pMS^3 mass spectrum of m/z 522.2711 → 279.1337 and thus, the loss of CO was assigned to the aldehyde moiety. Eventually, this evaluation supported the presumption of a hydroxyl group at the primary amine. Fourth, the CYP-mediated *N*-oxidation of primary

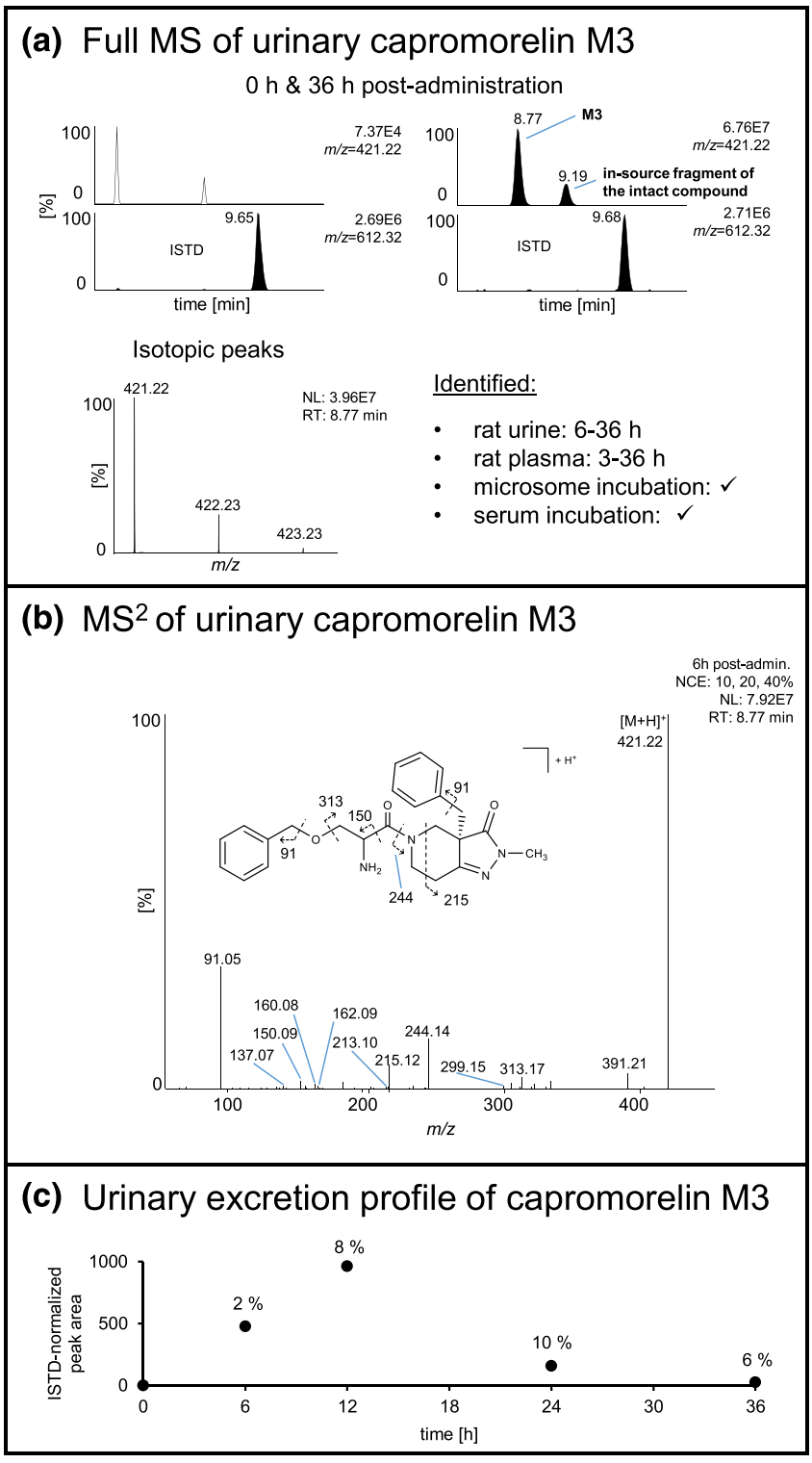

FIGURE 5 (a) The extracted ion chromatogram (mass tolerance ±5 ppm) of the full HRMS of the urinary capromorelin hydrolyzed M3 with the $[M + H]^+$ ion of m/z = 421.2234 at 0 and 36 h post-administration and, below, the isotope signals of the mass spectrum at t_R 8.77 min (36 h post-administration). (b) The MS^2 spectrum of the $[M + H]^+$ ion of a sample collected 6 h post-administration. (c) The urinary excretion profile with the indicated percentages referring to the relative abundance of the ISTD-normalized peak area

amines is a common phenomenon, reported, e.g., for phentermine, an aliphatic amine, or sulfamethoxazole, an aniline derivate, to respective hydroxylamine metabolites (Cribb & Spielberg, 1992; Duncan & Cho, 1982). It was further shown that hydroxylamine derivatives can autoxidize to nitroso (intermediate) and nitro derivatives (Hlavica & Damani, 1991). Consequently, it is conceivable that similar reaction sequences of the *N*-oxidation pathway for capromorelin occur as visualized in Figure S6. Indeed, the urinary capromorelin nitro M1–5 with the $[M + H]^+$ ion found at m/z = 536.2504 was observed at t_R 11.89 min and characterized by tMS^2 (Figure S7). In addition, the neutral loss of NO_2 could be tracked in the product ion scan mass spectra and by a neutral loss scan and precursor ion scan performed on a triple quadrupole MS (Figure S8). Sixth, within a period of almost 50 days and three freeze–thaw cycles, the capromorelin

post-administration samples of both rats (6 h) were analyzed. Interestingly, both of them clearly demonstrated a time-dependent relative decrease in the abundance of the hydroxylamine M1i, accompanied by an increase in intensity of the corresponding nitro M1–5 (Figure S9), most likely owing to autoxidation. Moreover, a corresponding $[M + H]^+$ ion at m/z = 520.2554, which could be assigned to the putative nitroso M1–4 (t_R 11.92 min), was identified at low abundance (MS^2 data not available). This observation was consistent with Naisbitt et al., who described the instability of a sulfamethoxazole nitroso metabolite owing to spontaneous reaction in solution (Naisbitt et al., 2002), further supporting the suggested formation of the capromorelin hydroxylamine M1i. However, the continuous chemical transformation of a metabolite is undesirable in sports drug testing and has to be taken into account for the (long-term) storage of a doping control sample. Nevertheless, it is one of the three major metabolites of capromorelin found in rat urine with the highest urinary concentration at 6 h post-administration and with a relative abundance of 3–5% over the total period of time compared to the unmodified compound (Figure 4c).

The second major metabolite was the capromorelin hydrolyzed M3, detected at t_R 8.77 min in rat urine 6–36 h post-administration, rat EDTA–plasma 3–36 h post-administration, human microsomes (*in vitro*) and human serum (*in vitro*) (Figure 5). The presence of this metabolite could be confirmed by tMS^2 experiment. The product ion spectrum of a 6 h post-administration rat sample of the $[M + H]^+$ ion at m/z = 421.2234 is shown in Figure 5b. The formation of this metabolite is not exclusive owing to the activity of amidases, since it was also observed in the enzyme blank control samples of both *in vitro* experiments with similar concentrations. The highest metabolite concentration excreted by rats was found at 12 h post-administration and the relative abundance over the total time compared with the unmodified compound was between 2 and 10% (Figure 5c).

The third major metabolite was suggested to represent the *N*-dealkylated capromorelin M4, detected at t_R 8.37 min in rat urine 6–36 h post-administration, rat EDTA–plasma 3–12 h post-administration, human microsomes (*in vitro*) and human serum (*in vitro*) (Figure S2a). Again, this metabolite was additionally observed in the *in vitro* enzyme blank control samples. *N*-Dealkylation of tertiary amines is catalyzed by cytochrome P450 enzymes (Iley & Tolando, 2000), and thus, high concentrations of M4 were found in rat urine. The metabolite was characterized by the product ion spectrum of the $[M + H]^+$ ion at m/z = 492.2605 of the 6 h post-administration rat urine sample as demonstrated in Figure S2b. Its maximum urinary concentration was found at 6 h post-administration and the relative abundance over the total time compared with the unmodified compound was between 4 and 6% (Figure S2c).

Briefly, the three predominant metabolites of capromorelin were predominantly found in rat urine and could all be detected from the start to the end of the sample collection period with relative abundances of 2–10%. The intact drug and the metabolite concentrations of the rat EDTA–plasma samples were significantly lower with approximately 2–3 orders of magnitude below the urinary concentration levels.

3.3 | Macimorelin

The interpretation of the full HRMS scan revealed 10 metabolites detected in rat urine (Figure 2b), zero metabolites in rat EDTA–plasma, seven metabolites detected in microsome-incubated drug samples and seven metabolites found after human serum incubation. Subsequent MS characterization and monitoring of the urinary excretion profile was accomplished for the most abundant metabolites observed in rat urine, which were proposed to represent mono-hydroxylated or epoxide M1c (Figure S13), *N*-dealkylated M2 (Figure 6) and M3 (Figure 7).

The CYP-mediated mono-hydroxylation or epoxidation revealed at least five metabolites eluting between t_R 6.30 and 7.33 min, detected in rat urine samples 6–24 h post-administration (Figure S13a). In order to determine the hydroxy or epoxide position in each compound, the four most abundant metabolites (t_R 6.30–7.02-min) were subsequently characterized by tMS^2 experiments and the respective product ion mass spectrum of the $[M + H]^+$ ion at m/z = 491.2401 and the indication of the most likely site of modification are depicted in Figure S14. Finally, M1c at t_R 6.83 min presented the highest relative abundances and was thus considered as a potential marker for sports drug testing approaches. The simultaneous presence in the enzyme blank control sample, although with an abundance four times less than observed in microsome-incubated samples, illustrates that microbial transformation or spontaneous and/or enzymatic oxidation could be involved in the formation of this metabolite. The results of the tMS^2 characterization minimized the possibilities of the available sites of metabolic reactions to the methyleneindole residue proximal to the 2-amino-2-methylpropanamide moiety as indicated in Figure S13b. This metabolite was primarily excreted after 6 h and the relative abundance was between 1 and 8% (Figure S13c).

The elimination of a tryptophan-like residue via C–N bond cleavage of macimorelin was proposed to yield two additional major metabolites, *N*-dealkylated macimorelin M2 (Figure 6) and macimorelin M3 (Figure 7). In the extracted ion chromatograms of the full HRMS scans of a rat urine sample collected 36 h post-administration, they were still clearly detected at t_R 4.62 min (M2) and t_R 4.16 min (M3). At t_R 7.89 min, two in-source-generated fragments of macimorelin were observed with identical $[M + H]^+$ ions for the two metabolites (not shown). Both metabolites were present in rat urine 6–36 h post-administration, but were not found in rat EDTA–plasma. In addition, M2 was found *in vitro*, although M3 was absent. Figure 6b shows the MS^2 spectrum of the $[M + H]^+$ ion at m/z = 289.1659 (M2) and Figure 7b shows the MS^2 spectrum of the $[M + H]^+$ ion at m/z = 187.0866 (M3); both spectra were acquired from a rat urine sample collected 12 h post-administration. M2 reached its maximum concentration at 12 h post-administration and the ISTD-normalized peak area at this time was more than three times higher than that of the intact compound (Figure 6c). Remarkably, this observation appeared to be even more significant for M3. While the shape of the excretion profile of M3 (Figure 7c) was similar to M2, the relative abundances at 12 and 24 h post-administration were two orders of magnitude higher than the intact compound's peak area.

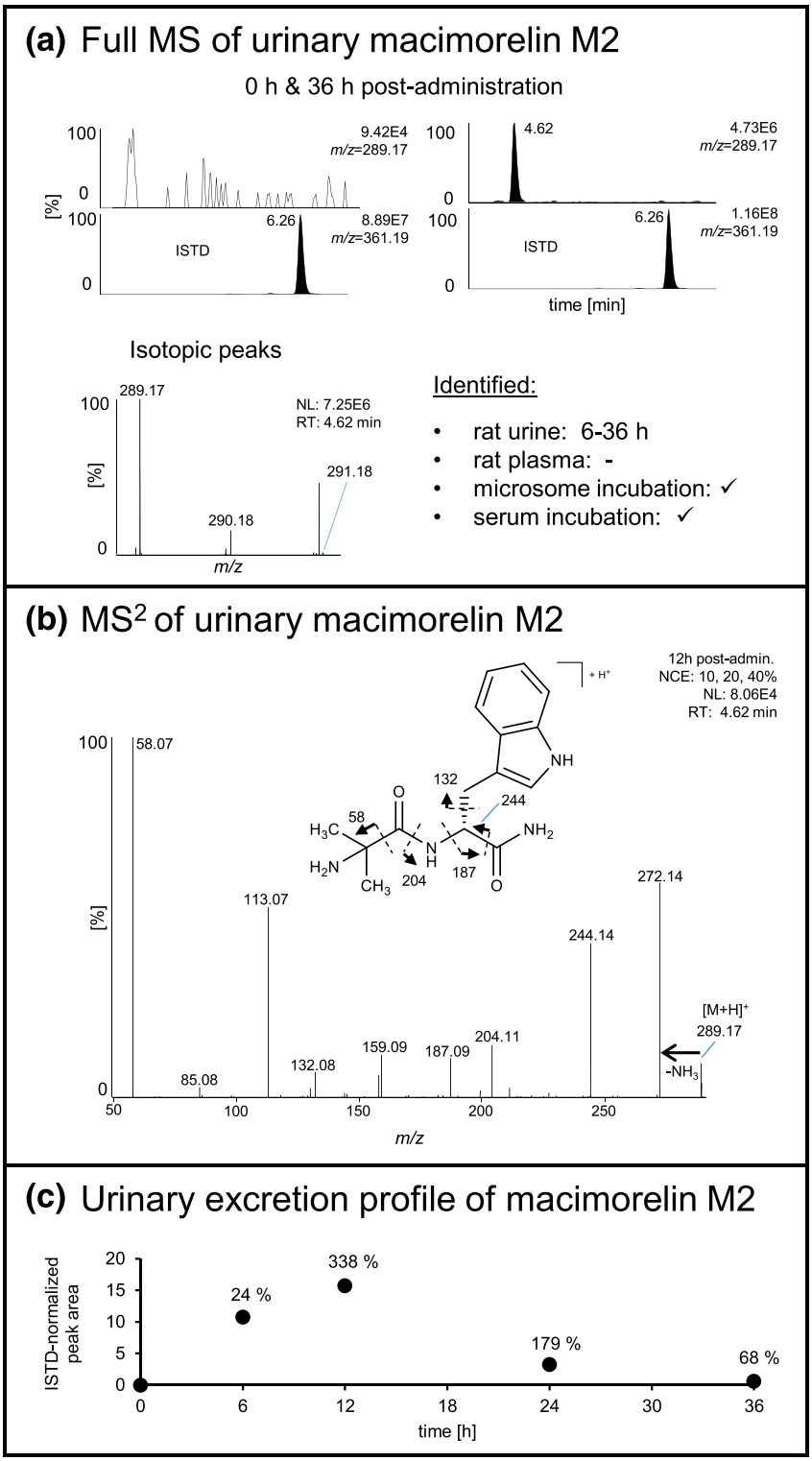

FIGURE 6 (a) The extracted ion chromatogram (mass tolerance ± 5 ppm) of the full HRMS of the urinary macimorelin *N*-dealkylated M2 with the $[M + H]^+$ ion of *m/z* 289.1659 at 0 and 36 h post-administration and, below, the isotope signals of the mass spectrum at t_R 4.62 min (36 h post-administration). (b) The MS^2 spectrum of the $[M + H]^+$ ion of a sample collected 12 h post-administration. (c) The urinary excretion profile with the indicated percentages referring to the relative abundance of the ISTD-normalized peak area

Briefly summarized, the three predominant metabolites of macimorelin were exclusively discovered in rat urine. High amounts of capromorelin M2 and M3 were observed over a presumably extended period of time exceeding the time of sample collection of this study. Moreover, the urinary concentration of macimorelin was sufficiently high to unambiguously detect it at any time up to 36 h post-administration. Although no metabolites were detected in rat EDTA–plasma, traces of the intact drug were found 3 h after the administration.

3.4 | Tabimorelin

The interpretation of the full HRMS scan revealed five metabolites detected in rat urine (Figure 2c), zero metabolites in rat EDTA–plasma, 10 metabolites detected in microsome-incubated drug samples and one metabolite detected after human serum incubation. Subsequent MS^2 characterization and monitoring the urinary excretion profile was accomplished for the predominant metabolite in

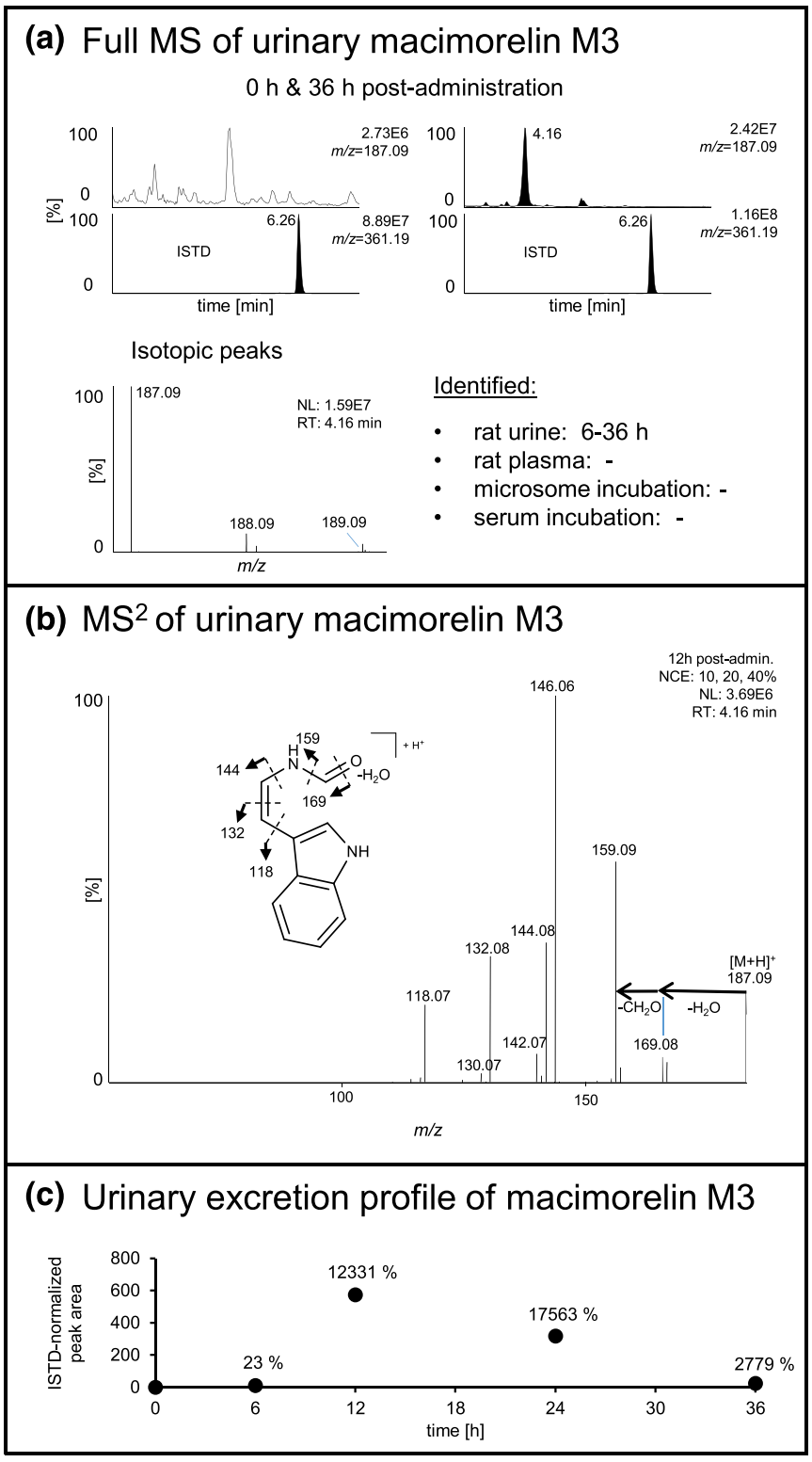

FIGURE 7 (a) The extracted ion chromatogram (mass tolerance ±5 ppm) of the full HRMS of the urinary macimorelin M3 with the $[M + H]^+$ ion of m/z = 187.0866 at 0 and 36 h post-administration and, below, the isotope signals of the mass spectrum at t_R 4.16 min (36 h post-administration). (b) the MS^2 spectrum of the $[M + H]^+$ ion of a sample collected 12 h post-administration. (c) The urinary excretion profile with the indicated percentages referring to the relative abundance of the ISTD-normalized peak area

rat, which was suggested to represent the *N*-glucuronidated M3-1 (Figure 8).

The tabimorelin phase II M3-1 was exclusively detected in rat urine from 6 to 24 h post-administration and could not be confirmed by any other *in vitro*/*in vivo* experiment. The compound eluted at t_R 8.65 min and the extracted ion chromatogram of the $[M + H]^+$ ion at m/z 707.3651 is shown in Figure 8a. The metabolite was characterized by a tMS^2 experiment and its product ion mass spectrum of a rat urine sample 6 h post-administration is provided in Figure 8b. M3-1 was primarily excreted at 6 h post-administration and the relative abundance was found to be between 0 and 2% (Figure 8c). Other studies suggested a significantly decreased *N*-glucuronidation of drugs

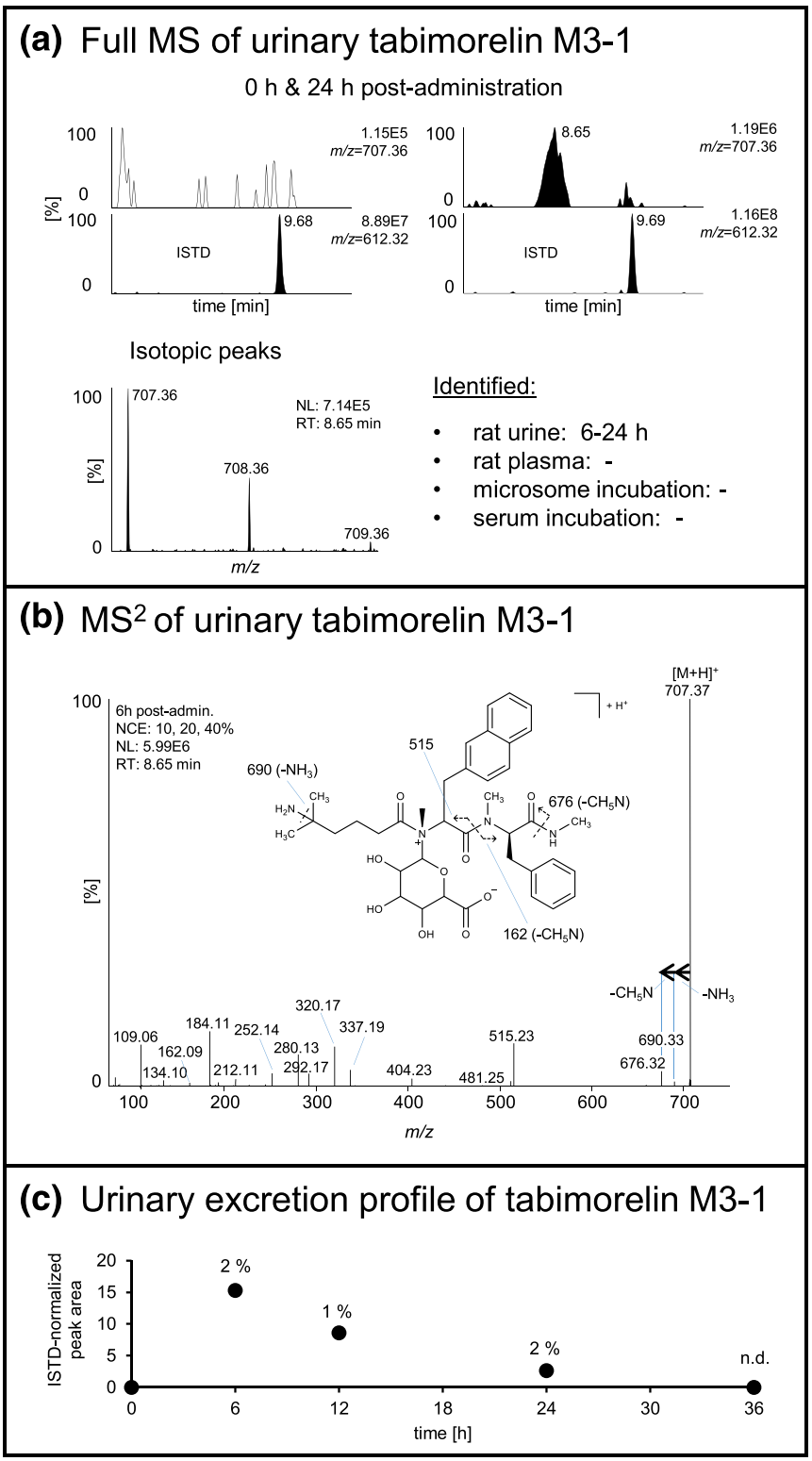

FIGURE 8 (a) the extracted ion chromatograms (mass tolerance ±5 ppm) of the full HRMS of the urinary tabimorelin *N*-glucuronidated M3-1 with the $[M + H]^+$ ion of m/z = 707.3579 at 0 and 24 h post-administration and, below, the isotope signals of the mass spectrum at t_R 8.65 min from a sample collected 24 h post-administration. (b) The MS^2 spectrum of the $[M + H]^+$ ion of a sample collected 6 h post-administration. (c) The urinary excretion profile with the indicated percentages referring to the relative abundance of the ISTD-normalized peak area

in rat compared with human (Kaji & Kume, 2005; Miles et al., 2005). This metabolite seems promising for human doping control purposes. No other metabolite achieved the minimum required 1% of relative abundance that would entail further characterizations at this point. In contrast to the few urinary metabolites observed for tabimorelin, the intact drug was traceable in both rat urine and rat EDTA–plasma by the end of sample collection. However, the concentration levels of the intact compound of rat EDTA–plasma samples were significantly lower by approximately three orders of magnitude below the urinary concentration levels.

3.5 | Method characterization and validation

In order to deter doping using the three new compounds, namely capromorelin, macimorelin and tabimorelin, it was desirable to establish a WADA-validated anti-doping test. Owing to their physicochemical properties, the substances were implemented into an existing routine initial test method, which also covers other GHRPs/GHS analytes, such as alexamorelin, GHRP-2 or anamorelin. This screening was devised for the detection of GH-releasing factors, which are peptides and peptide-related compounds (<2 kDa), in human urine (Goergens, Guddat, Thomas, & Thevis, 2018). A second detection method for human EDTA–plasma was validated in the same manner. The results of the method validation are summarized in Table 2. For initial testing purposes, the selectivity was demonstrated by analyzing 10 different blank samples (female, *n* = 5 and male, n = 5). No interfering signals were identified in either urine or plasma. The repeatability of six different urine samples or plasma samples, expressed in rt_R (%), was between 0.05 and 0.37% and thus below the required <1%. For urinary matrix, the assessment of carryover after analyzing a blank sample after a sample containing a high concentration of the analyte (400% MRPL) revealed no carryover for tabimorelin and macimorelin, and a minor carryover of 0.1% for capromorelin. For EDTA–plasma matrix, no carryover was observed for any of the analytes. The LOD of the analytes was estimated at between 0.17 and 0.45 ng/ml (urine) and between 0.02 and 0.60 ng/ml (EDTA–plasma).

The occurrence of a presumptive adverse analytical finding can be confirmed in three different CP methods depending on the matrix and the choice of sample preparation as described in Section 2. Regardless of the procedure or sample matrix, all CP assays showed excellent selectivity after analyzing 10 different blank samples. Robustness was evaluated by analyzing six different urine samples with a concentration of 50% MRPL (SPE sample preparation) or 100% MRPL (D&I and PP), prepared on another day. The rt_R (%) of all test batches was between 0.07 and 0.57% and thus considered to be robust. No carryover was observed and LOI was estimated at between 0.46 and 0.89 ng/ml for urine direct injection (D&I), between 0.18 and 0.41 ng/ml for urine after SPE sample preparation and between 0.19 and 0.89 ng/ml for plasma matrix via PP.

In clinical studies, maximum plasma concentrations of 29 ng/ml (tabimorelin; Zdravkovic et al., 2003), 30–250 ng/ml (capromorelin; Ellis et al., 2015) and 0.9–7.6 ng/ml (macimorelin; Piccoli et al., 2007) were reached after single or multiple oral doses of the drugs. Thus, sensitive analytical testing in the range of pharmacologically relevant drug concentrations can be performed with the EDTA–plasma assays presented here.

TABLE 2 Results of the qualitative initial testing procedure (ITP) and confirmation procedure (CP) validation for human urine and human EDTA–plasma matrix

ITP for urine (D&I) and plasma (PP) samples						
Compound	**tSIM ion 1**	**tSIM ion 2**	**Selectivity (*n* = 10)**	**Repeatability rt_R (RSD, %) (*n* = 6)**	**Carryover (%) (*n* = 1)**	**LOD (ng/ml) (*n* = 6)**
Tabimorelin	529.3173	530.3201	OK (D&I)	0.19 (D&I)	0.0 (D&I)	0.30 (D&I)
			OK (PP)	0.10 (PP)	0.0 (PP)	0.60 (PP)
Macimorelin	475.2442	476.2477	OK (D&I)	0.21 (D&I)	0.0 (D&I)	0.45 (D&I)
			OK (PP)	0.05 (PP)	0.0 (PP)	0.18 (PP)
Capromorelin	506.2762	507.2795	OK (D&I)	0.37 (D&I)	0.1 (D&I)	0.17 (D&I)
			OK (PP)	0.08 (PP)	0.0 (PP)	0.02 (PP)
CP for urine (D&I), urine (SPE) and plasma (PP) samples						
Compound	**tMS^2 ion 1**	**tMS^2 ion 2**	**tMS^2 ion 3**	**Selectivity (*n* = 10)**	**Robustness rt_R (RSD, %) (*n* = 6)**	**Carryover (%) (*n* = 1)**	**LOI (ng/ml) (*n* = 6)**
Tabimorelin	184.1120	252.1382	212.1073	OK (D&I)	0.12 (D&I)	0.0 (D&I)	0.64 (D&I)
				OK (SPE)	0.12 (SPE)	0.0 (SPE)	0.18 (SPE)
	280.1331	184.1120	252.1382	OK (PP)	0.12 (PP)	0.0 (PP)	0.89 (PP)
Macimorelin	113.0714	159.0916	244.1446	OK (D&I)	0.12 (D&I)	0.0 (D&I)	0.89 (D&I)
				OK (SPE)	0.57 (SPE)	0.0 (SPE)	0.41 (SPE)
	272.1394	289.1659	159.0916	OK (PP)	0.07 (PP)	0.0 (PP)	0.19 (PP)
Capromorelin	244.1448	245.1484	215.1179	OK (D&I)	0.46 (D&I)	0.0 (D&I)	0.46 (D&I)
				OK (SPE)	0.11 (SPE)	0.0 (SPE)	0.19 (SPE)
	244.1448	263.1390	215.1179	OK (PP)	0.08 (PP)	0.0 (PP)	0.19 (PP)

tMS^2 ions upper row (urine assays) and tMS^2 ions lower row (plasma assay).
D&I, "Dilute-and-inject"; tSIM, targeted SIM; LOD, limit of detection; LOI, limit of identification.

4 | CONCLUSION

In sports drug testing, the primary analysis matrices are urine and blood. As soon as new substances emerge and an illegal use in sports cannot be excluded, these compounds require a detailed characterization and appropriate analytical detection methods must be provided immediately. The missing information about the metabolic conversion and excretion pathway of the short-lived ghrelin mimetics capromorelin, macimorelin and tabimorelin are of particular interest as they could improve the sensitivity, specificity and detection window of a detection assay. Indeed, combining distinct pre-analytical and computational techniques (*in vitro*/*in vivo*/*in silico*), several metabolites of capromorelin, macimorelin and tabimorelin were observed and thoroughly characterized by LC–HRMS/MS. Notwithstanding, the rather nonpeptidic precursor compounds were not subjected to proteolytic degradation, unlike other peptide ghrelin receptor agonists, such as GHRPs, and while various proteolytic metabolites exhibited comparable or increased relative abundances (Semenistaya et al., 2015), this observation was the exception here. Thus, most of the metabolites were less concentrated than their precursor compounds with relative abundances <10%, both in urine and in blood. Nonetheless, in the case of an adverse analytical finding, they might be of importance to complement the confirmation of identity of the ghrelin mimetic. Furthermore, macimorelin M2 and macimorelin M3 were detected with substantially elevated urinary excretion levels compared with the intact compound. Based on the assumption that metabolic conversions are transferable from rat model to human, these metabolites are highly valuable as they are likely to increase sensitivity, specificity and detection windows. In addition, macimorelin M3 could prove to be a useful longer-term metabolite, as it still remained with significantly higher relative concentration by the end of urine sample collection. Finally, in accordance with the WADA guidelines, the commercially available intact substances (in contrast to their metabolites) were incorporated into initial testing procedures (LOD 0.02–-0.60 ng/ml) and confirmation procedures (LOI 0.18–0.89 ng/ml) for human urine and blood matrix.

FUNDING

The study was carried out with support of the Manfred Donike Institute for Doping Analysis (Cologne, Germany), the World Anti-Doping Agency (Montreal, Canada, #18A03MT) and the Federal Ministry of the Interior, Building and Community of the Federal Republic of Germany (Bonn, Germany).

Open access funding enabled and organized by Projekt DEAL.

CONFLICT OF INTEREST

The authors declare no conflict of interest.

ORCID

Mario Thevis https://orcid.org/0000-0002-1535-6451

REFERENCES

Cordido, F., Isidro, M. L., Nemina, R., & Sangiao-Alvarellos, S. (2009). Ghrelin and growth hormone secretagogues, physiological and pharmacological aspect. *Current Drug Discovery Technologies*, *6*(1), 34–42. https://doi.org/10.2174/157016309787581048

Cribb, A. E., & Spielberg, S. P. (1992). Sulfamethoxazole is metabolized to the hydroxylamine in humans. *Clinical Pharmacology and Therapeutics*, *51*(5), 522–526. https://doi.org/10.1038/clpt.1992.57

Djoumbou-Feunang, Y., Fiamoncini, J., Gil-de-la-Fuente, A., Greiner, R., Manach, C., & Wishart, D. S. (2019a). BioTransformer: A comprehensive computational tool for small molecule metabolism prediction and metabolite identification. *Journal of Cheminformatics*, *11*(1), 2. https://doi.org/10.1186/s13321-018-0324-5

Djoumbou-Feunang, Y., Pon, A., Karu, N., Zheng, J., Li, C., Arndt, D., … Wishart, D. S. (2019b). CFM-ID 3.0: Significantly improved ESI–MS/MS prediction and compound identification. *Metabolites*, *9*(4), 72. https://doi.org/10.3390/metabo9040072

Duncan, J. D., & Cho, A. K. (1982). *N*-Oxidation of phentermine to *N*-hydroxyphentermine by a reconstituted cytochrome P-450 oxidase system from rabbit liver. *Molecular Pharmacology*, *22*(2), 235–238.

Ellis, A. G., Zeglinski, P. T., Brown, D. J., Frauman, A. G., Millard, M., & Furness, J. B. (2015). Pharmacokinetics of the ghrelin agonist capromorelin in a single ascending dose phase-I safety trial in spinal cord-injured and able-bodied volunteers. *Spinal Cord*, *53*(2), 103–108. https://doi.org/10.1038/sc.2014.218

Esposito, S., Deventer, K., Geldof, L., & Van Eenoo, P. (2015). *In vitro* models for metabolic studies of small peptide hormones in sport drug testing. *Journal of Peptide Science*, *21*(1), 1–9. https://doi.org/10.1002/psc.2710

Fitch, W. L., He, L., Tu, Y. P., & Alexandrova, L. (2007). Application of polarity switching in the identification of the metabolites of RO9237. *Rapid Communications in Mass Spectrometry*, *21*(10), 1661–1668. https://doi.org/10.1002/rcm.3009

Goergens, C., Guddat, S., Thomas, A., & Thevis, M. (2018). Recent improvements in sports drug testing concerning the initial testing for peptidic drugs (< 2 kDa)—Sample preparation, mass spectrometric detection, and data review. *Drug Testing and Analysis*, *10*, 1755–1760. https://doi.org/10.1002/dta.2503

Guan, F., You, Y., Li, X., & Robinson, M. A. (2019). A comprehensive approach to detecting multitudinous bioactive peptides in equine plasma and urine using HILIC coupled to high resolution mass spectrometry. *Drug Testing and Analysis*, *11*, 1308–1325. https://doi.org/10.1002/dta.2671

Hansen, B. S., Raun, K., Nielsen, K. K., Johansen, P. B., Hansen, T. K., Peschke, B., … Ankersen, M. (1999). Pharmacological characterisation of a new oral GH secretagogue NN703. *European Journal of Endocrinology*, *141*(2), 180–189. https://doi.org/10.1530/eje.0.1410180

Hlavica, P., & Damani, L. A. (1991). *N-Oxidation of drugs: Biochemistry, pharmacology, toxicology* (pp. 207–215). Midsomer Norton: Springer Science + Business Media Dordrecht.

Iley, J., & Tolando, R. (2000). The oxidative dealkylation of tertiary amides: Mechanistic aspects. *Journal of the Chemical Society, Perkin Transactions*, *2*(11), 2,328–2,336. https://doi.org/10.1039/B001756F

Judak, P., Grainger, J., Goebel, C., Van Eenoo, P., & Deventer, K. (2017). DMSO assisted electrospray ionization for the detection of small peptide hormones in urine by dilute-and-shoot–liquid-chromatography–high resolution mass spectrometry. *Journal of the American Society for Mass Spectrometry*, *28*(8), 1657–1665. https://doi.org/10.1007/s13361-017-1,670-7

Kaji, H., & Kume, T. (2005). Characterization of afloqualone *N*-glucuronidation: Species differences and identification of human UDP–glucuronosyltransferase isoform(s). *Drug Metabolism and Disposition*, *33*(1), 60–67. https://doi.org/10.1124/dmd.104.001925

Kim, Y., Jeon, M., Min, H., Son, J., Lee, J., Kwon, O. S., & Kim, K. H. (2018). Development of a multi-functional concurrent assay using weak cation-exchange solid-phase extraction (WCX–SPE) and reconstitution with a diluted sample aliquot for anti-doping analysis. *Rapid Communications in Mass Spectrometry*, *32*(11), 897–905. https://doi.org/10.1002/rcm.8119

Knights, K. M., Stresser, D. M., Miners, J. O., & Crespi, C. L. (2016). *In vitro* drug metabolism using liver microsomes. *Current Protocols in Pharmacology*, *74*, 7–8. https://doi.org/10.1002/cpph.9

Kwok, K. Y., Choi, T. L. S., Kwok, W. H., Lau, M. Y., Leung, E. M. K., Leung, G. N. W., … Ho, E. N. M. (2020). Detection of bioactive peptides including gonadotrophin-releasing factors (GnRHs) in horse urine ursing ultra-high performance liquid chromatography–high resolution mass spectrometry (UHPLC/HRMS). *Drug Testing and Analysis*, *12*, 1274–1286. https://doi.org/10.1002/dta.2880

Lange, T., Thomas, A., Walpurgis, K., & Thevis, M. (2020). Fully automated dried blood spot sample preparation enables the detection of lower molecular mass peptide and non-peptide doping agents by means of LC–HRMS. *Analytical and Bioanalytical Chemistry*, *412*, 3765–3777. https://doi.org/10.1007/s00216-020-02634-4

Miles, K. K., Stern, S. T., Smith, P. C., Kessler, F. K., Ali, S., & Ritter, J. K. (2005). An investigation of human and rat liver microsomal mycophenolic acid glucuronidation: Evidence for a principal role of UGT1A enzymes and species differences in UGT1A specificity. *Drug Metabolism and Disposition*, *33*(10), 1513–1520. https://doi.org/10.1124/dmd.105.004663

Miller, R. R., Doss, G. A., & Stearns, R. A. (2004). Identification of a hydroxylamine glucuronide metabolite of an oral hypoglycemic agent. *Drug Metabolism and Disposition*, *32*(2), 178–185. https://doi.org/10.1124/dmd.32.2.178

Moulin, A., Ryan, J., Martinez, J., & Fehrentz, J. A. (2007). Recent developments in ghrelin receptor ligands. *ChemMedChem*, *2*(9), 1242–1259. https://doi.org/10.1002/cmdc.200700015

Naisbitt, D. J., Farrell, J., Gordon, S. F., Maggs, J. L., Burkhart, C., Pichler, W. J., … Park, B. K. (2002). Covalent binding of the nitroso metabolite of sulfamethoxazole leads to toxicity and major histocompatibility complex-restricted antigen presentation. *Molecular Pharmacology*, *62*(3), 628–637. https://doi.org/10.1124/mol.62.3.628

Okano, M., Sato, M., Ikekita, A., & Kageyama, S. (2010). Determination of growth hormone secretagogue pralmorelin (GHRP-2) and its metabolite in human urine by liquid chromatography/electrospray ionization tandem mass spectrometry. *Rapid Communications in Mass Spectrometry*, *24*(14), 2046–2056. https://doi.org/10.1002/rcm.4619

Piccoli, F., Degen, L., MacLean, C., Peter, S., Baselgia, L., Larsen, F., … Drewe, J. (2007). Pharmacokinetics and pharmacodynamic effects of an oral ghrelin agonist in healthy subjects. *The Journal of Clinical Endocrinology and Metabolism*, *92*(5), 1814–1820. https://doi.org/10.1210/jc.2006-2,160

Pugliese, J., Boyce, M. C., Lawler, N. G., Coumbaros, J., & Le, T. T. (2019). Dispersive SPE, an alternative to traditional SPE for extraction of 43 doping peptides from equine urine prior to LC–MS screening. *Forensic Toxicology*, *38*(2), 365–377.

Qi, X., Wu, B., Cheng, Y., & Qu, H. (2009). Simultaneous characterization of pyrrolizidine alkaloids and *N*-oxides in *Gynura segetum* by liquid chromatography/ion trap mass spectrometry. *Rapid Communications in Mass Spectrometry*, *23*(2), 291–302. https://doi.org/10.1002/rcm.3862

Ramanathan, R., Su, A. D., Alvarez, N., Blumenkrantz, N., Chowdhury, S. K., Alton, K., & Patrick, J. (2000). Liquid chromatography/mass spectrometry methods for distinguishing *N*-oxides from hydroxylated compounds. *Analytical Chemistry*, *72*(6), 1352–1359. https://doi.org/10.1021/ac9911692

Rhodes, L., Zollers, B., Wofford, J. A., & Heinen, E. (2018). Capromorelin: A ghrelin receptor agonist and novel therapy for stimulation of appetite in dogs. *Veterinary Medicine and Science*, *4*(1), 3–16. https://doi.org/10.1002/vms3.83

Semenistaya, E., Zvereva, I., Thomas, A., Thevis, M., Krotov, G., & Rodchenkov, G. (2015). Determination of growth hormone releasing peptides metabolites in human urine after nasal administration of GHRP-1, GHRP-2, GHRP-6, hexarelin, and ipamorelin. *Drug Testing and Analysis*, *7*(10), 919–925. https://doi.org/10.1002/dta.1787

Sobolevsky, T., & Ahrens, B. (2020). High-throughput liquid chromatography tandem mass spectrometry assay as initial testing procedure for analysis of total urinary fraction. *Drug Testing and Analysis*. https://doi.org/10.1002/dta.2917

Svensson, J., Monson, J. P., Vetter, T., Hansen, T. K., Savine, R., Kann, P., … Group, N. N. C. R. (2003). Oral administration of the growth hormone secretagogue NN703 in adult patients with growth hormone deficiency. *Clinical Endocrinology*, *58*(5), 572–580. https://doi.org/10.1046/j.1365-2265.2003.01754.x

Thomas, A., Delahaut, P., Krug, O., Schaenzer, W., & Thevis, M. (2012). Metabolism of growth hormone releasing peptides. *Analytical Chemistry*, *84*(23), 10252–10259. https://doi.org/10.1021/ac302034w

Thomas, A., Delahaut, P., Krug, O., Schänzer, W., & Thevis, M. (2012). Metabolism of growth hormone releasing peptides. *Analytical Chemistry*, *84*(23), 10252–10259. https://doi.org/10.1021/ac302034w

Thomas, A., Goergens, C., Guddat, S., Thieme, D., Dellanna, F., Schaenzer, W., & Thevis, M. (2016). Simplifying and expanding the screening for peptides <2 kDa by direct urine injection, liquid chromatography, and ion mobility mass spectrometry. *Journal of Separation Science*, *39*(2), 333–341. https://doi.org/10.1002/jssc.201501060

Thomas, A., Hoeppner, S., Geyer, H., Schaenzer, W., Petrou, M., Kwiatkowska, D., … Thevis, M. (2011). Determination of growth hormone releasing peptides (GHRP) and their major metabolites in human urine for doping controls by means of liquid chromatography mass spectrometry. *Analytical and Bioanalytical Chemistry*, *401*(2), 507–516. https://doi.org/10.1007/s00216-011-4,702-3

Thomas, A., Knoop, A., Schanzer, W., & Thevis, M. (2017). Characterization of *in vitro* generated metabolites of selected peptides <2 kDa prohibited in sports. *Drug Testing and Analysis*, *9*(11–12), 1799–1803. https://doi.org/10.1002/dta.2306

Timms, M., Hall, N., Levina, V., Vine, J., & Steel, R. (2014). A high-throughput LC–MS/MS screen for GHRP in equine and human urine, featuring peptide derivatization for improved chromatography. *Drug Testing and Analysis*, *6*(10), 985–995. https://doi.org/10.1002/dta.1624

WADA. (2015). Minimum criteria for chromatographic–mass spectrometric confirmation of the identity of analytes for doping control purposes. https://www.wada-ama.org/en/resources/science-medicine/td2015idcr

WADA. (2019a). Anti-doping testing figures. Retrieved from https://www.wada-ama.org/en/resources/laboratories/anti-doping-testing-figures-report

WADA. (2019b). The World Anti-Doping Code. International Standard for Laboratories January. https://www.wada-ama.org/sites/default/files/resources/files/isl_nov2019.pdf

WADA. (2020). The World Anti-Doping Code. International Standard. Prohibited List. https://www.wada-ama.org/sites/default/files/wada_2020_english_prohibited_list_0.pdf

White, H. K., Petrie, C. D., Landschulz, W., MacLean, D., Taylor, A., Lyles, K., … Capromorelin Study, G. (2009). Effects of an oral growth hormone secretagogue in older adults. *The Journal of Clinical Endocrinology and Metabolism*, *94*(4), 1198–1206. https://doi.org/10.1210/jc.2008-0632

Zaretzki, J., Matlock, M., & Swamidass, S. J. (2013). XenoSite: Accurately predicting CYP-mediated sites of metabolism with neural networks. *Journal of Chemical Information and Modeling*, *53*(12), 3373–3383. https://doi.org/10.1021/ci400518g

Zdravkovic, M., Olsen, A. K., Christiansen, T., Schulz, R., Taub, M. E., Thomsen, M. S., … Ilondo, M. M. (2003). A clinical study investigating the pharmacokinetic interaction between NN703 (tabimorelin), a potential inhibitor of CYP3A4 activity, and midazolam, a CYP3A4 substrate. *European Journal of Clinical Pharmacology*, *58*(10), 683–688. https://doi.org/10.1007/s00228-002-0539-1

Zvereva, I., Semenistaya, E., Krotov, G., & Rodchenkov, G. (2016). Comparison of various *in vitro* model systems of the metabolism of synthetic doping peptides: Proteolytic enzymes, human blood serum, liver and kidney microsomes and liver S9 fraction. *Journal of Proteomics*, *149*, 85–97. https://doi.org/10.1016/j.jprot.2016.08.016

SUPPORTING INFORMATION

Additional supporting information may be found online in the Supporting Information section at the end of this article.

How to cite this article: Lange T, Thomas A, Görgens C, et al. Comprehensive insights into the formation of metabolites of the ghrelin mimetics capromorelin, macimorelin and tabimorelin as potential markers for doping control purposes. *Biomedical Chromatography*. 2021;e5075. https://doi.org/10.1002/bmc.5075